International Journal of Nanoelectronics and Materials
Volume 14 (Special Issue) August 2021 [439-456]

Characterisation of Mechanical-Electrical Properties of Graphene Nanoplatelets Filled Epoxy as Conductive Ink in Various Patterns

Aina Natasha Hosnie[1], Mohd Azli Salim[1,2,3*], Nor Azmmi Masripan[1,2,3], Adzni Md. Saad[1,3], Feng Dai[4], Azmi Naroh[4] and Mohd Nizam Sudin[1]

[1]Fakulti Kejuruteraan Mekanikal, Universiti Teknikal Malaysia Melaka (UTeM), Malaysia
[2]Advanced Manufacturing Centre, Universiti Teknikal Malaysia Melaka (UTeM), Malaysia
[3]Intelligent Engineering Technology Services Sdn. Bhd., No.1, Jalan TU43, Taman Tasik Utama, 76450 Ayer Keroh, Melaka, Malaysia
[4]Institute of Science and Technology, China Railway Eryuan Engineering Group Co.Ltd, No.3 Tongjin Road, Sichuan, 610031, P.R.China.
[4]Department of Mechanical Engineering, Politeknik Ungku Omar, Malaysia

ABSTRACT

Graphene is one of conductive material that has been studied widely other than silver in the printed electronics industry. This material is considered as "wonder material" which has excellent properties in conducting electricity. Due to these properties advantageous of graphene, a new research study had been conducted regarding the electrical and mechanical properties of Graphene Nanoplatelets (GNPs) conductive ink in various print patterns. The way properties of graphene affecting the current flow of ink had become one of the objectives of this study with respect to hardness and sheet resistivity ink. On the other hand, this study aimed to determine the most excellent pattern and width that good in conducting electicity. Based on the existing formulation of graphene-based conductive ink, this study combined three different materials which are Graphene Nanoplatelets as a filler, epoxy resin as a binder, and polytheramine as a hardener. Samples of the ink were patterned into four (4) different types, which are a straight-line, zigzag, sinusoidal, and square pattern, and three (3) different widths, which are 1 mm, 2 mm, and 3 mm. In this study, to achieve the objectives, two tests were conducted, which are the sheet resistivity test by using a four-point probe and hardness test by using a nanoindenter. At the end of this study, sample of ink that have low sheet resistivity and high hardness has good properties among others samples and vice versa. Besides that, the best pattern that had the high performance of graphene was determined and discussed. The findings of this study will be used in the future and be very helpful in improving the performance of the existing conductive ink, which can efficiently conduct electricity at a low cost of production.

Keywords: conductive ink, graphene ink, hardness, polymer epoxy resin, sheet resistivity

1. INTRODUCTION

Conductive ink is a mature field that is now being spun out into commercial applications and has been widely used in the electronic area. Conductive ink is a technology that combines the utility of ink with the ability to conduct electricity through formulation. Basically, the formulation of ink is the process of depositing the conductive nanomaterial by combining it with a non-conductive material, which naturally enables the flow of electrons to pass through the ink [1]. The nanomaterial is a small-scale chemical substance with a nanostructure that can reach 1 nm (10-9 m) [2]. A lot of nanomaterials have been employed in conductive ink formulation such as gold (Au) [3], copper (Cu) [4], carbon, and newly, graphene [5,6]. Recently, graphene (GR) is undergoing intensive study in the conductive field as it is considered a "wonder material" that

* Corresponding Author: azli@utem.edu.my

provides excellent properties in conducting electricity [7]. The Graphene shows extremely promising high functionality as a conductive material in terms of electrical, mechanical, and thermal properties [8,9]. According to Zhu and Chen [10], the use of GR as a filler in the composites of ink offered many advantages due to its high mobility electron [11]. Besides that, the past study of the properties GR had reported about the flexible properties of GR as a printed ink [12]. In this study, GR was patterned into various types of patterns without affecting the properties of the ink. Even though the ability of GR holds a significant promise to enhance the electrical properties, the effort to produce low-cost formulation ink remains unsuccessful due to the high cost of GR [13].

A lot of studies had been conducted to minimize the use of GR. For instance, the recent research on the charge percolation in metal-organic frameworks (MOFs) through the formulation of composites with Graphene (GR) had provided insights into high electrically conductive of composites beyond 30 wt% of GR [14]. In this study, the prototypal graphene-based of MOFs called HKUST-1 was composited with several of G content, which was attained through the sol-gel method. The experiment started with the reading of HKUST-1 conductivity at $\sigma = 2*10\text{-}8$ Sm-1 where the conductivity increased up to 23.3 Sm-1 with an increase of various GR until 59.4 wt%. As a result, the variation of GR loading affected the measurement of electrical conductivity and the presence of charge percolation detected at the lowest filler loading of 30 wt%. On the other hand, there was a study, which reported about the structural, chemical, and electrical characterization of conductive graphene-polymer composites film [15]. This study used a few methods to gain results such as scanning electron microscopy (SEM), atomic force microscopy (AFM), Raman spectrometry, X-ray photoelectron spectroscopy (XPS), and time-of-flight secondary ion mass spectrometry (ToF-SIMS). With the systematic analysis, the study resulted that the dispersions of GR in the film can be affected by the type of GR powder used and affected the electrical performance of the composites. The result of the study concluded that Graphene Nanoplatelets (GNPs) are the most suitable nanomaterial to be used for the formulation of ink.

In the present research, there is a proposed study regarding the percolation effects on Graphene Nanoplatelets (GNPs) conductive ink in various print patterns. In the conductive ink study, many factors do affect the performance of printed ink, and one of the significant factors is electrical percolation. In line with this, it is important to determine how the percolation affects the current flow in ink and this matter has become one of the objectives of this study. On the other hand, one of the factors that give huge differences regarding the performance GNPs in conducting electricity along with the ink is the pattern of the printed ink. Due to this matter, this study aims to determine the best pattern in conducting electricity in relation to the percolation of GNPs. Based on the existing formulation of conductive ink, this research is using GNPs as a filler, epoxy resin as a binder, and polytheramine as a hardener [16-20].

2. MATERIAL AND METHODS

2.1 Stage 1: Samples Preparation of Graphene-Based Conductive Ink

The methodology of the research started with the sample preparation of the ink involving three (3) main processes, which are the formulation of ink that is standardized from the previous study, printing process, and curing process.

2.1.1 Formulation Process

In this study, the experimental approach started with the formulation of the graphene-based conductive ink. The combination of filler, binder, and hardener was the basic materials used in the study of conductive ink. The filler is the most important material for the composition

process because of its ability to conduct electricity. This study was carried out by using Graphene Nanoplatelets (GNPs) as the filler for the composite in order to increases the bulk, viscosity, and firmness of the composite. GNPs has been proven as one of the best conductor materials in this conductive ink technology as it has a high capability to conduct electricity and has good properties as a conductor.

On the other hand, this study decided to use Bisphenol A diglycidyl ether (BADGE or DGEBA), which is a constituent of epoxy resins as a binder. In this study, the DGEBA epoxy resin is made up of epichlorohydrin and bisphenol-A with an average molecular density of ≤ 700 g/mol. The density of the resin is 1.168 g/ml, with a viscosity value in the range of 500-750 mPa.s at 25 °C. This colorless resin was purchased from Sigma Aldrich, with the trade name of Araldite 506 Epoxy Resin. Binder plays an important role in binding the particles of each material together and turns into a composite. The DGEBA is a thermosetting group of polymers that is usually used as a binder, which can greatly influence the mechanical properties of the Electrically Conductive Adhesive (ECA). On the other hand, the use of a hardener in this experiment was to solidify the composite of the combination between filler and binder. Since this type of polymer are two-component adhesives, therefore, a hardener was required to complete the curing process via the cross-linking process. The Hunstman polyetheramine D230 hardener was used, which is an amine group type of curing agent. The density of the curing agent is 0.947 g/ml with a viscosity of 9 mPa.s at 25 °C.

A combination of filler, binder, and hardener was standardized with a constant ratio along with the experiment. Table 1 represents the formulation ratio of the graphene-based conductive ink that was chosen based on a previous study. In 2019, a study related to the formulation of graphene-based ink had concluded that 30 % to 40 % of filler loadings were the most preferable ratios compared to the other percentages. This was due to the existence of electrical conductivity had been shown to start from 30 wt % of filler loadings. Hence, the current study chooses the optimum filler loading of 35 % wt in the formulation process.

Table 1 Formulation of graphene-based conductive ink

Sample	Filler		Binder		Hardener (g)	Total (g)
	(%)	(g)	(%)	(g)		
1	35	0.7	65	1.3	0.39	2.39

Based on the formulation stated in Table 1, sample preparation started by taking out the materials from the chemical storage cabinet. The materials used for sample preparation, which are GNPs (filler), DGEBA epoxy resin (binder), and the hardener. The masses of the material were weighed using an analytical balance, which is a highly sensitive automatic machine in measuring the mass of the materials. In order to switch on the analytical balance, the power button at the adapter needs to be pressed. Before weighting the materials, the analytical machine must be calibrated by leveling the adjustment feet. Next, the door of the machine was opened to place the empty container inside the machine chamber (refer to Figure 1). Then the door was closed and the "tare" button was pressed. The machine read zero mass for the container after a few seconds.

After eliminating the weight of the container, the door of the balance was opened again, and the material was weighed depending on the formulation. When the balance displayed the reading of the needed weight, the process of adding the material was stopped. This process was repeated for other materials. After the process of weighing the materials finished, it was proceeded by the mixing process.

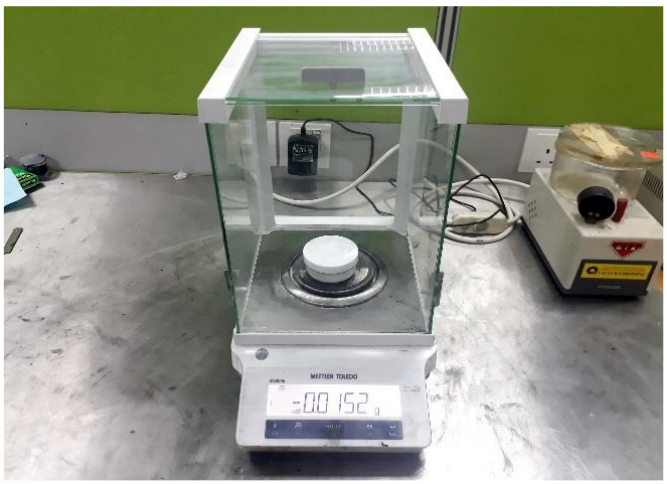

Figure 1. Container inside the weight balance.

The mixing process was done by mixing the weighted materials into one container. The materials were blended and stirred until they formed a rough composite. After that, the container filled with composite and container holder were combined and put together in the balance machine. The balance read the weight of the container and the container holder. This weight was used for the calibration of the Thinky mixer. By referring to Figure 2 (a), the mixer was opened and the container holder was put inside the mixer at 45° of tilt angle. The mixer must be calibrated before starting the mixing process by setting the weight balance based on the weight of the container and container holder that had been weighted before as shown in Figure 2 (b). This process was continued by setting the time and speed at the display of the mixer at 3 minutes and 2000 rpm. The mixer was closed and the "start" button was pressed. After 3 minutes, the container holder was taken off. Figure 3 shows the difference before and after the use of the Thinky mixer.

(a) (b)

(b) **Figure 2.** Calibration which is (a) container inside the mixer and (b) weight balance.

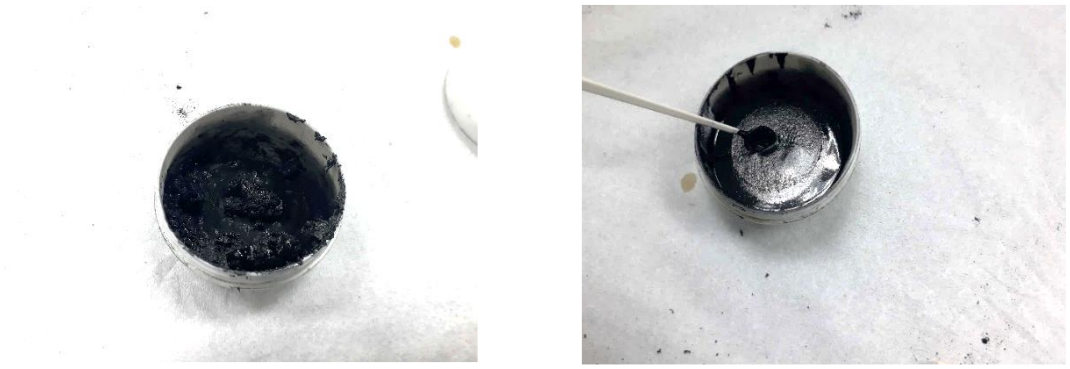

(a) (b)

Figure 3. (a) Before the mixing process and (b) after the mixing process.

2.1.2 Printing and Curing Processes

After the material preparation, the procedural steps were continued with the printing process. For this study, the printing process was carried out in various widths and patterns of the samples. The implemented concept of the printing process was a casting method with the help of a doctor-blade technique. The casting process is usually used with a liquid composite by putting it into the mold of the desired shape and the doctor-blade technique is used to place the wet composite into the mold properly. This doctor blade is a widely used technique in producing a thin film on the substrates. In this study of the material behavior and properties, after the material preparation was done, the composite had to go through a printing process. The printing process started by gluing together the composite with the TPU substrate at the lower surface of the mold with the tape.

Firstly, the TPU substrate must be cleaned with acetone to avoid any small particles that can damage the surface of the ink after the curing process. After the TPU substrate had been glued together with the mold, the mold position was changed upside down. The wet composite was placed on the top of the mold and the doctor-blade technique was applied. Figure 4 shows how the doctor-blade technique works. When the wet composite had been put on the top of the mold surface, the blade started to move constantly towards the direction as shown in Figure 5. The movement of this blade was controlled manually. This doctor-blade was used to give a lot of pressure on the wet composite for it to spread into the mold according to the shape. This technique also produced less space for air or bubbles in the wet composite. After the printing process was done, the TPU substrates were taken off from the bottom of the mold. This process was executed slowly in order to avoid the ink sticking to the mold. The sample was considered to fail if the wet composite did not take off from the mold. This printing process was repeated two times for each pattern and width.

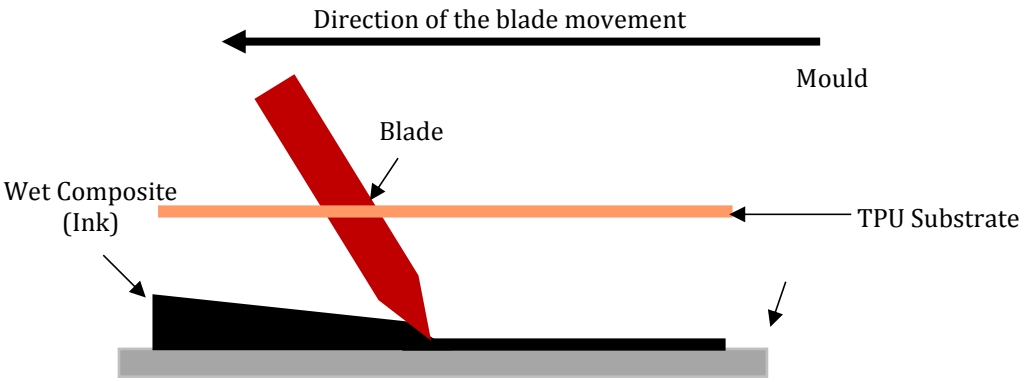

Figure 4. Doctor-blade technique.

The curing process was performed after the printing process was done. The aim of this curing process is to cure the wet composite and turns it into a composite that has high-strength bonds. After the printing process, the samples underwent a curing process by putting the samples on the tray and placed them into the oven. This curing process had been set for 30 minutes at 100 °C of the temperature. This process also makes the wet composite to grow in a high-temperature environment. After 30 minutes, the tray was taken out from the oven and the samples were cooled down by using natural air. These samples were then marked with five-point markers for the test as shown in Figure 5.

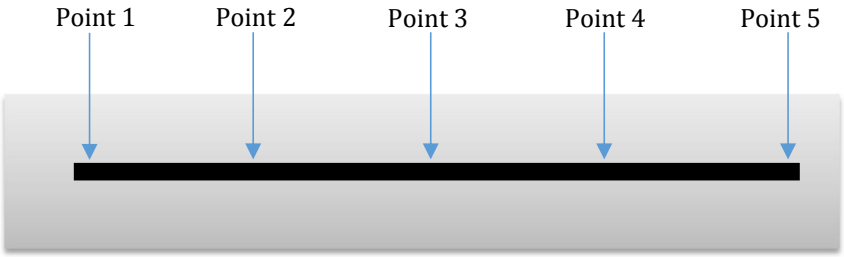

Figure 5. The point marker location of the sample.

2.2 Stage 2: Experimental Study

In this study of graphene-based conductive ink, two (2) tests were conducted to achieve the objectives. The tests were resistivity and voltage test by 4-point probe and hardness test by nanoindenter. Resistivity can be described as the material resistance to the flow of electricity in the electrical circuit. Sheet resistivity was obtained using a four-point probe machine due to its independence of the square and the low resistivity of the thin film. The past study had stated that material with low resistivity has the ability to conduct electricity easily. Hardness Vickers is the measurement of hardness value in the micro size of the specimen. The graphene-based conductive ink samples underwent the micro-hardness test to investigate the ability of the material to resist local plastic deformation by standardized loading. The hardness of each sample was measured by applying a constant load of 6 mN during the test.

2.2.1 Resistivity Test

In this study, the readings of the voltage and resistivity on the conductive ink were obtained by using the 4-point probe machine. The test started by switching on the machine and setting up the voltmeter of the machine. This square meter must be cleared from the previous data to avoid any continued data in the software. To clear the previous data, the button 'Enter' was pressed for around 5 seconds to erase the previous data from the voltmeter memory. The personal computer (PC) was connected to this Jandel machine software, as the data was logging into this software automatically. In this study, the value of current had been set at 10μA and applied for all the samples. After the setup process was done, the sample was put on the base under the probe as shown in Figure 6.

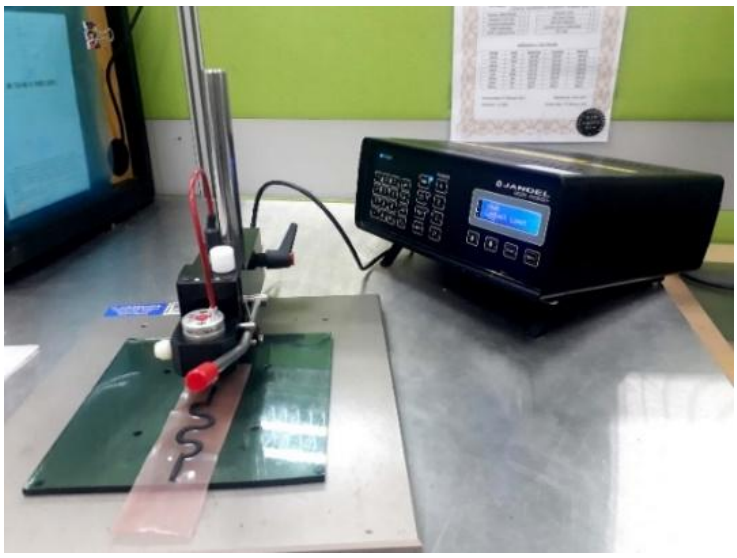

Figure 6. The Four-Point probe.

This test was performed by adjusting the position of the cylindrical probe near the surface of the sample by using the twirl lever beside the cylindrical probe. Before the cylindrical probe was moved, there was a gap between the probe and the sample. By moving the cylindrical probe, it touched the sample surface. It was performed by pulling the twirl lever down until the cylindrical probe touched the surface of the sample. When the probe touched the surface of the sample, the voltmeter read and displayed the voltage of the sample in millivolt (mV) and resistivity in ohm/sq (Ω/sq). The data at the voltmeter was saved by logging it into the software automatically. By entering the 'enter' button, data was logged into the software. After that, the data was exported into a folder.

2.2.2 Hardness Test

The samples also underwent a hardness test by using the nanoindenter machine. Based on this test, the data on the hardness of the composite can be obtained. This hardness test is important to determine the flexibility properties of the conductive ink. To start the hardness test, the sample was placed on the mechanical stage of the nanoindenter. For the adjustment, it was done manually as shown in Figure 7. In order to make sure the data can be read clearly, the sample was put in focus and at the right position.

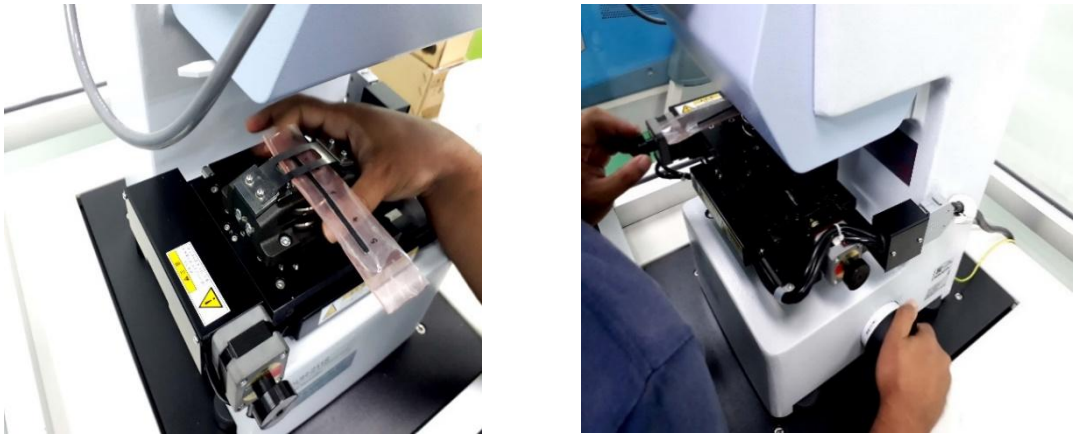

(a) (b)

Figure 7. Hardness test which is (a) sample on the machine (b) reposition the sample.

3. RESULTS AND DISCUSSION

3.1 Electrical Properties

In the present work, a study on the electrical properties in terms of sheet resistance had been performed. The objectives of the electrical properties study are to measure the sheet resistance of the graphene-based printed ink from three different widths and to determine the influence of the different widths on the electrical property of the ink. Sheet resistance can be described as a fundamental property of a material that quantifies how strongly it resists or conducts electrical current, which is inverse to the electrical conductivity. Sheet resistance test was performed using the four-point probe machine due to its independence of the square and low resistivity of the thin film. During the experiment, a constant current, I went through the outer two probes to measure the R_S of a sample, and the reading of V was recorded based on the voltage, V drop between the inner two probes. The sheet resistance was calculated based on the area that the current went through and the resistivity of the sample material. For a very thin sample where thickness, t is smaller than probe spacing, s ($t < s$) ring protrusion of current emanates from the probes. With the superposition of the current, the relation of sheet resistance, R_S with the resistivity, ρ and cross-sectional area, A is calculated by:

$$R_s = \frac{L}{A} \tag{1}$$

According to the expression of the sheet resistance of a sample, L is the length of the tested area, and the unit for R_S is ohm per square (Ω/sq). The cross-section of the probe area is a measurement based on the square shape, which includes width and thickness. Based on this, the cross-sectional area is replaced with width and thickness as shown below:

$$R_s = \rho \frac{L}{\omega t} \tag{2}$$

where w is represented as width and t as the thickness of the probes that go in the sample.
Length, width, and thickness measure sheet resistance in the direction of length cross-section with width and thickness. The length is considered equal to the width ($L = w$) as both are in the same direction. By applying the same conditions of ($L = w$) in Eq. 2, the equation of the sheet resistance can be expressed as:

$$R_s = \frac{\rho}{t} \tag{3}$$

By referring to the objective of the study, which is to identify the electrical properties of the graphene-based conductive ink, the sheet resistance equation is used to point out the relationship between the resistivity and thickness. Based on the equation, the sheet resistance is directly proportionally to resistivity and in contrast with thickness. In this study of conductive ink, the results from the experiments were analyzed according to two different characteristics, which are pattern and width. As stated in the methodology, the conductive ink was patterned in four different types (straight-line, zigzag, sinusoidal, and square) and three different widths (3 mm, 2 mm, and 1 mm). In order to figure out which pattern and width are the most efficient in conducting electricity, the analysis was done as the following discussion in the next sub-chapter. The sheet resistance is one of the electrical properties that reflects the capability of ink samples in conducting electricity. Table 2 illustrates the value of R_S in micro value for graphene-based ink samples with four different patterns and three different widths. Each sample consists of five points on the top of the sample's surface to ensure the measurement of R_S had been taken uniformly. From the data, the lowest value of R_S indicates the functionality of ink in allowing current to flow through the samples and vice versa.

Table 2 The sheet resistance values for graphene-based ink samples

Width	Sheet Resistance, R_S (μΩ/sq)			
	Straight Line	**Zigzag**	**Sinusoidal**	**Square**
1 mm	12.74	11.77	7.60	7.59
	8.12	18.28	13.91	10.42
	7.01	18.15	12.35	12.82
	9.08	12.53	10.36	16.00
	6.64	10.41	14.59	12.62
2 mm	6.83	11.02	12.07	13.54
	6.06	15.39	10.00	9.81
	8.70	9.49	10.01	13.63
	7.22	15.99	8.76	9.49
	6.05	14.63	9.42	9.49
3 mm	5.41	10.71	6.96	7.56
	6.62	11.97	7.22	7.48
	5.63	8.39	5.48	6.74
	4.98	13.55	5.80	7.78
	7.65	9.73	6.83	10.44

Generally, the average value of the zigzag pattern is slightly higher compared to the straight-line, sinusoidal, and square patterns. According to this, Figure 8 shows that the graph of sheet resistance against points taken for 1 mm width of samples to ease the interpretation of data. As shown, the zigzag pattern visually represents the higher value of R_S, which illustrates a sudden spike in point 2 and 3 at 18.38 μΩ/sq and 18.12 μΩ/sq. However, the solid line of the straight line shows the constantly lower values compared to other patterns starting from point 2 to point 5 (below 9.08 μΩ/sq) while point 1 is slightly higher at 12.74 μΩ/sq. For sinusoidal and square samples, both patterns start at the lower values of average R_S around 7.59 μΩ/sq to 7.60

μΩ/sq approximately and ending at 14.59 μΩ/sq and 12.62 μΩ/sq. Based on the illustrated line graphs, the increase in the value of R_S is basically due to the width of the samples, and the complexity of the designed pattern.

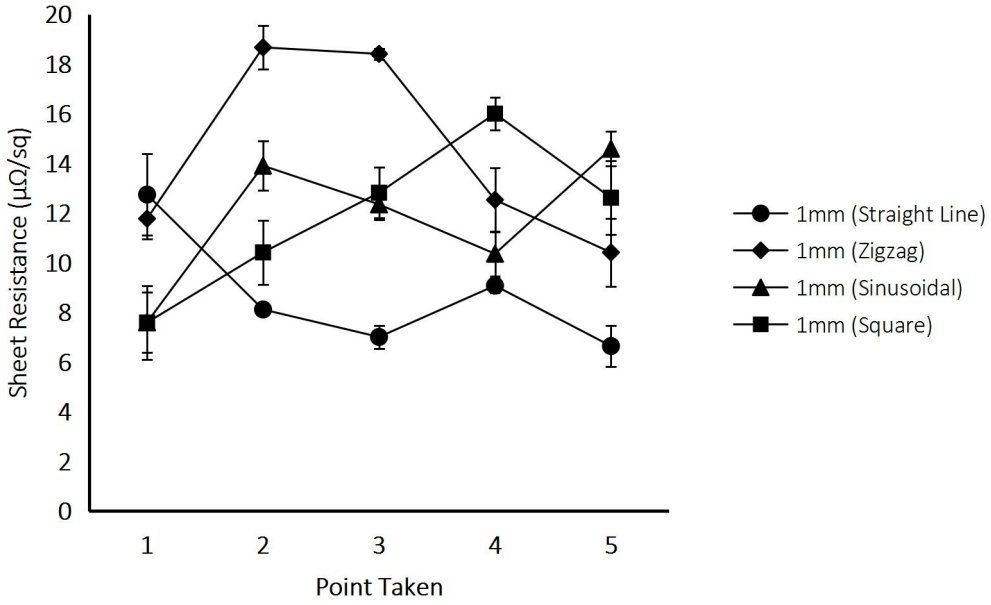

Figure 8. Sheet resistance against point taken (width: 1 mm).

Figure 9 shows that the graph of sheet resistance against point taken for 2 mm of width. All the five points of straight-line relatively have the lowest values. However, while the values of straight-line maintain as the lowest, zigzag shows a fluctuating trend. It starts with a low value at 11.77 μΩ/sq and rises at 18.28 μΩ/sq and continue to fall and rise to point 5. For sinusoidal and square patterns, the values of R_S are vice versa with the trends of 1 mm width samples as both patterns start at higher values and continuously fall until point 5 at 9.42 μΩ/sq and 9.49 μΩ/sq. On the other hand, Figure 10 indicates that the graph of sheet resistance against point taken for 3 mm width samples. Generally, values for 3 mm samples maintain the same level in the range of 4 μΩ/sq to 10 μΩ/sq except for the zigzag pattern. The zigzag pattern shows a fluctuating trend of the line graph and stays as the highest values for all five points between 8 μΩ/sq to 14 μΩ/sq.

Overall, the analysis based on the width of the samples shows that the straight-line pattern has the lowest values of sheet resistance for all widths, and the zigzag shows the highest values. Sinusoidal and square patterns stay in the middle of the straight line and zigzag for all three widths with the fluctuating trend of line graphs. According to this, a straight-line pattern proves that it can allow electricity to flow in the ink better than others due to the simplicity of design as compared to zigzag. Besides that, there is the possibility that the ink is not well distributed all over the mold that was used to print the samples as the doctor-blade technique was conducted manually and the inconstant blade movement affected the distribution works. Moreover, the high viscosity of the composite causes difficulties to perform the printing procedure in compliance with the texture of the ink. Thus, it causes the inconsistent thickness of printed inks on the glass side. Some regions may have different thickness, which leads to different spreads of conducting material.

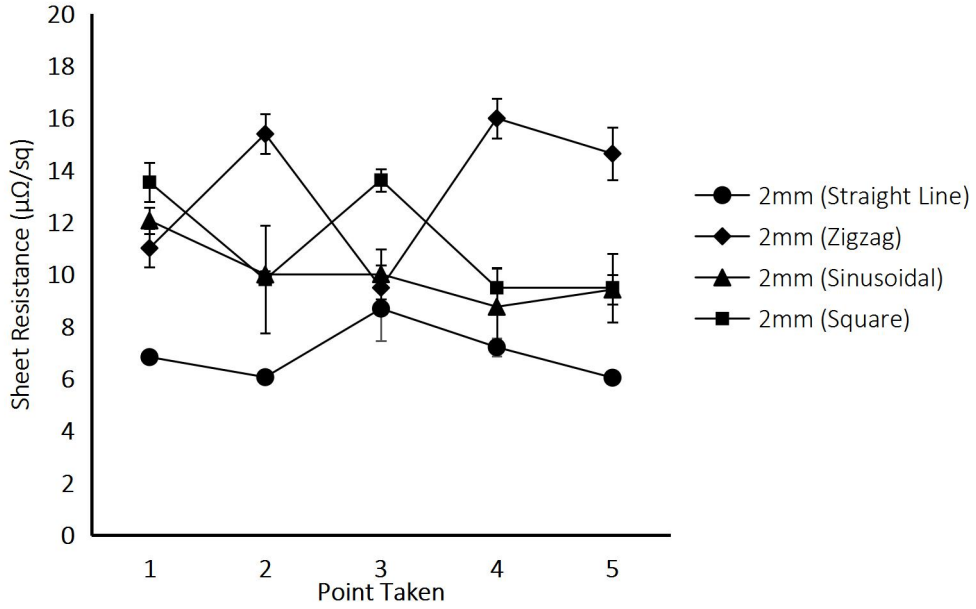

Figure 9. Sheet resistance against point taken (width: 2 mm).

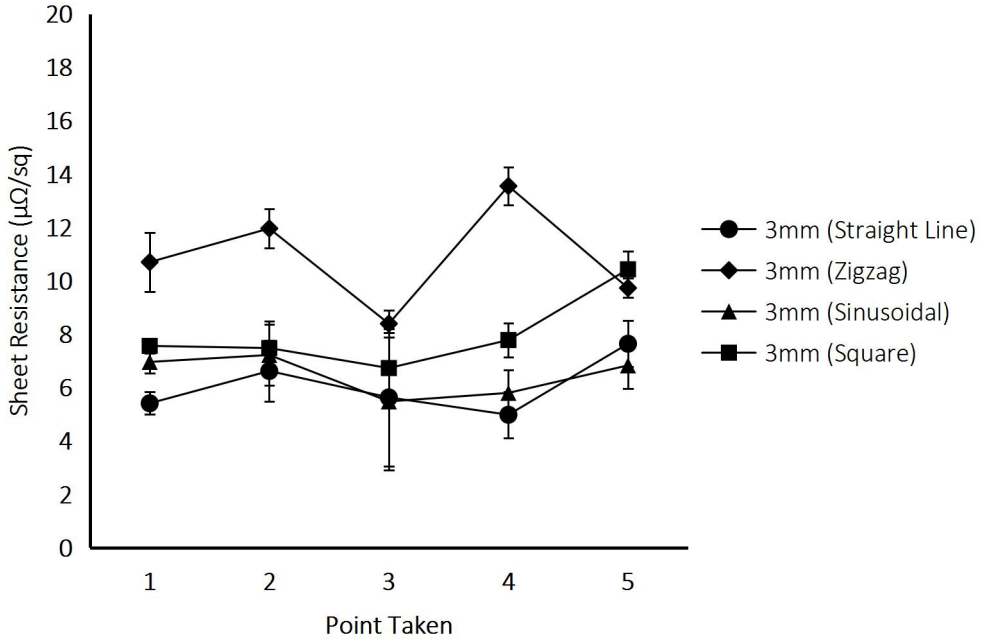

Figure 10. Sheet resistance against point taken (width: 3 mm).

Figure 11 shows that the results of straight-line on width against five points taken during the experiment. From the observation of the sheet resistance graph, 1mm has the highest value in the range between 6 to 12 μΩ/sq while 3mm shows the lowest plotted line graph. On the other hand, 2mm line graph maintain in the middle samples with the value from 6 μΩ/sq to 8 μΩ/sq. Besides that, the results of the zigzag pattern (refer to Figure 12) show some differences in sheet resistance results compared to the straight-line pattern. In the R_S graph, 1mm stay as the highest average values while 2mm as at a moderate plotted line with an average values 9 μΩ/sq

to 15 μΩ/sq. The 3mm values are illustrated as the lowest line graph with a fluctuating trend. Based on the results for the sinusoidal pattern (refer to Figure 13), the 2mm sample has moderate values for sheet resistivity. Based on the graph in Figure 14, the reading for 1mm is decreased rapidly from point 1 until point 3 and increased slightly at point 4 while the 2mm sample shows a little bit different in average resistivity reading which in the range from 9 μΩ/sq to 3 μΩ/sq. The reliability of the data on sample 1 and sample 2 show slightly different except at points 1 and 5 which the error bar has a bigger gap. From the graph, the average resistivity values for 2mm is higher at point 3 while lower value at point 5.

Based on the discussion, it can conclude that width results show some inconsistency regarding the sheet resistance. Graphene-based conductive ink shows that 1mm width has higher resistivity compared to 3mm width. This shows that the wider the size of samples the lower the value of resistivity due to the wider the width of the sample, it has low resistance which makes the flow of current in the ink more efficient compared to the small width. Besides that, there is the possibility that the agglomeration effect happened on the ink samples which lead to high resistivity reading [17]. Furthermore, 1 mm samples are difficult to print in the form of the wet composite which leads to damage on the surface of ink during the curing process. In sheet resistance study, thickness plays an important role in controlling the resistance in the printed ink. This is due to the probes of the four-point probe read the sheet resistance values based on the thickness of the samples. As discussed before, during the printing process there is the possibility that the ink is not well distributed along with the mold and might cause damage to the samples. Even though 1mm thickness applied to all samples due to distribution issues the samples might be less than 1mm especially for 1mm width samples. Based on this probe read 1mm width as the highest values for sheet resistance as the thickness of samples might be less than 1 mm.

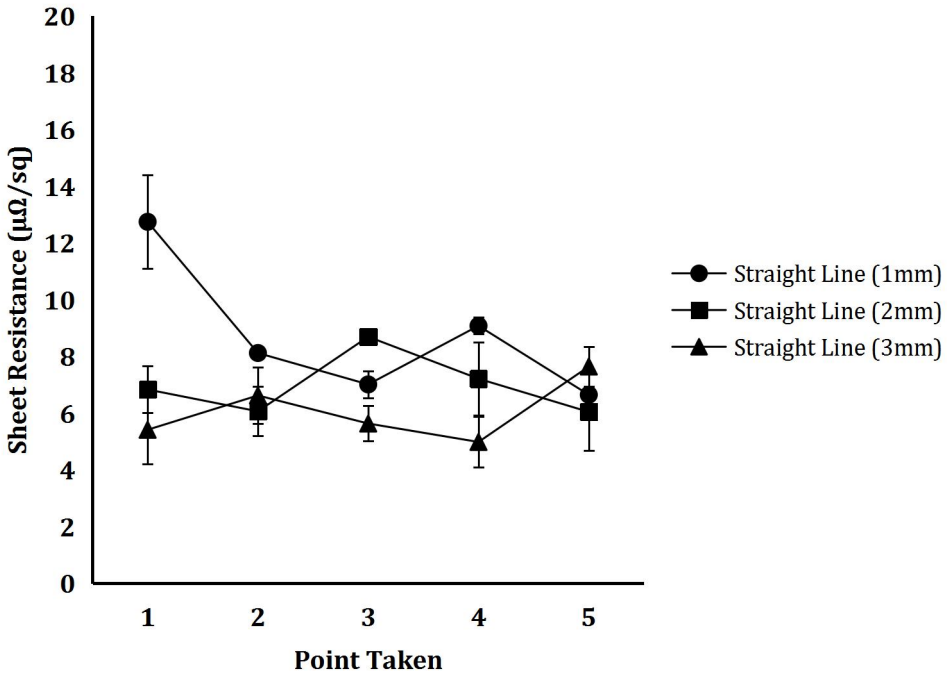

Figure 11. Sheet resistance against point taken (pattern: straight-line).

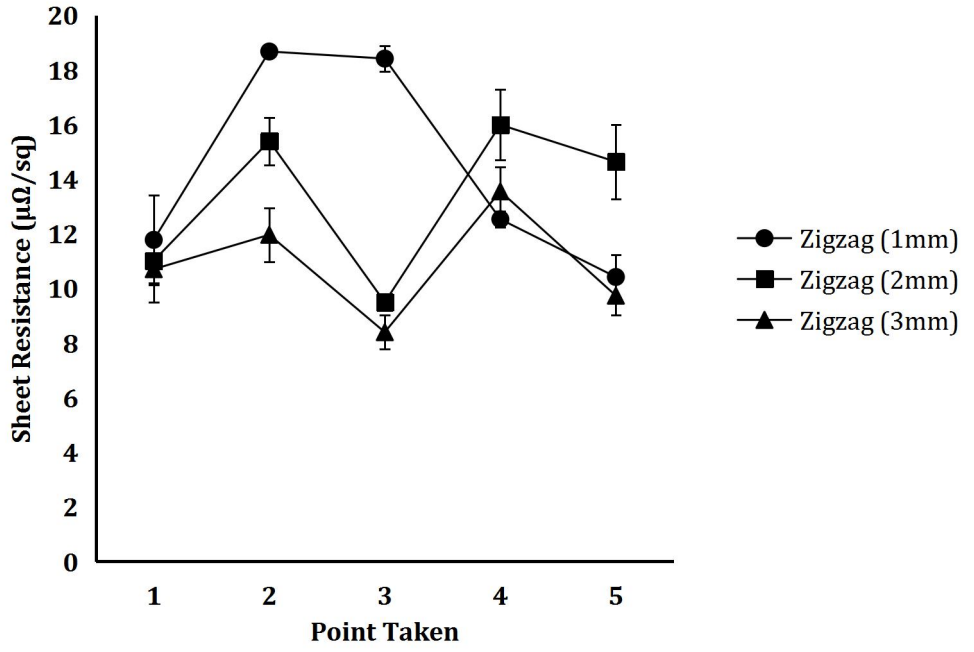

Figure 12. Sheet resistance against point taken (pattern: zigzag).

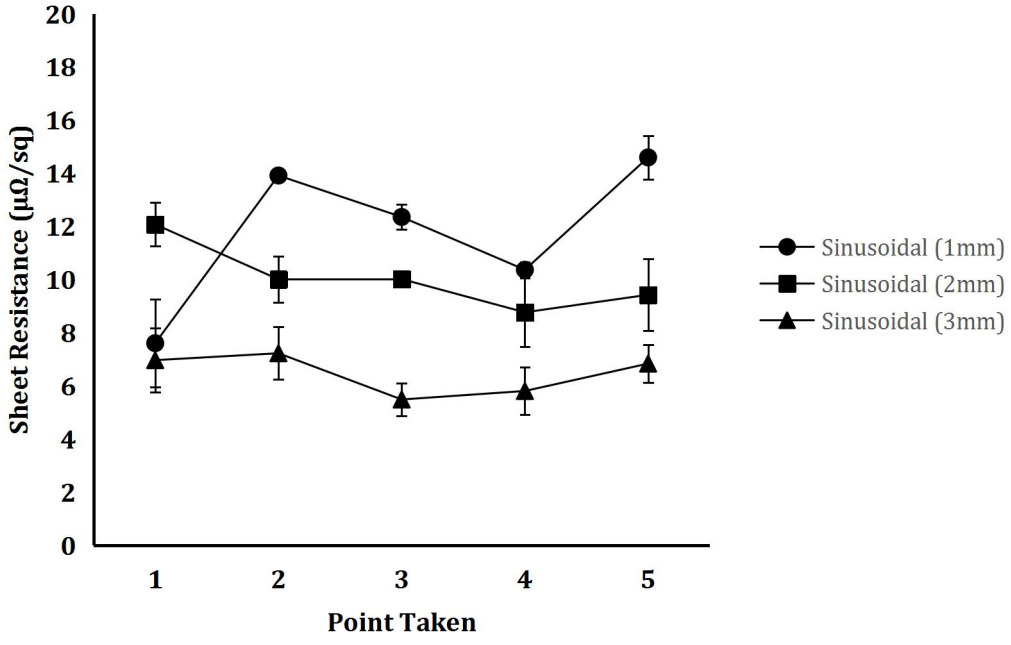

Figure 13. Sheet resistance against point taken (pattern: sinusoidal).

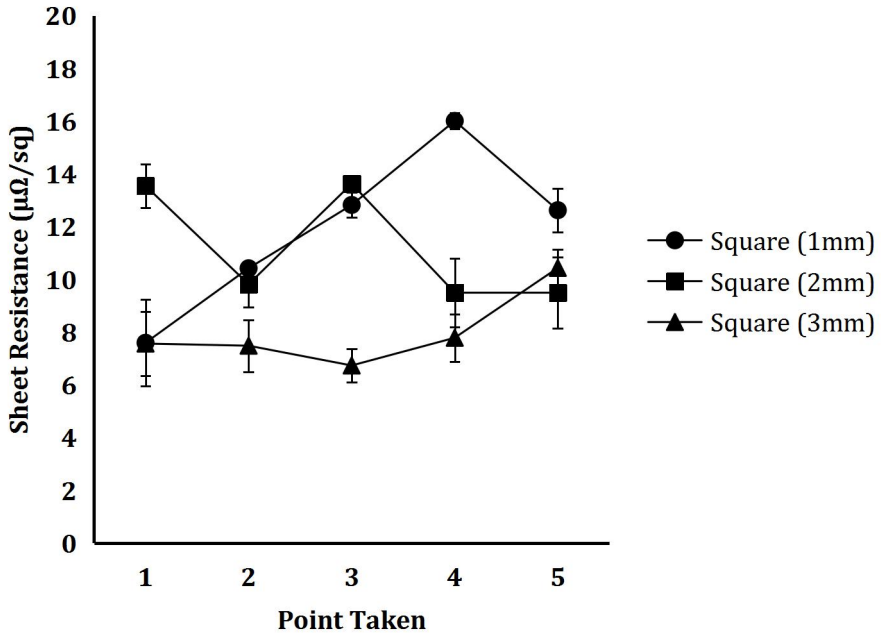

Figure 14. Sheet resistance against point taken (pattern: square).

3.2 Hardness Test

In this study, the graphene-based conductive ink samples underwent the micro-hardness test to investigate the ability of the material to resist local plastic deformation by standardized loading. The hardness of each sample was measured with a constant applied load of 6 mN during the test. The findings in this test are been tabulated, and to simplify the results of this micro-hardness test the data has been illustrated in the form of a graph and shown in Table 3.

Table 3 The hardness values for graphene-based ink samples

Width	Sheet Resistance, R_s (μΩ/sq)			
	Straight-line	Zigzag	Sinusoidal	Square
1 mm	0.38	0.23	0.18	0.80
	0.68	0.11	0.30	0.13
	0.86	0.06	0.58	0.26
	0.55	0.37	0.34	0.19
	0.19	0.59	0.09	0.73
2 mm	2.78	2.55	2.18	1.91
	3.22	2.71	2.12	1.69
	3.13	1.79	3.37	1.06
	2.49	2.46	2.86	2.28
	2.86	2.24	2.38	1.70
3 mm	3.85	4.20	3.70	2.91
	3.96	2.51	3.27	2.74

3.12	2.74	4.24	3.32
2.78	2.28	4.13	3.22
3.05	3.74	3.06	2.62

From the observation of the hardness test, there are variations in hardness values due to the different contents of the hardener in the ink. Graphene has excellent mechanical properties, particularly high Young's modulus. These exceptional properties make graphene an ideal candidate as a filler for nanocomposites materials. This Graphene ink is aimed to be exploited due to the remarkable mechanical enhancement effect with the possibility to introduce further functionalities such as electrical conductivity. For this study, nanoindentation analysis was carried out using the method described by [14]. Two frequently measured mechanical properties are Young's modulus and hardness. As the indenter is driven into the material, both elastic and plastic deformations cause the formation of hardness. After the indenter is withdrawn, only the elastic portion of the displacement is recovered, thus this recovery enables one to determine the elastic properties of a material. Therefore, the first step of measurement was preparing the sample by mounting it on a sample disk. The load-displacement graph shows the typical load-indentation depth curve obtained by nanoindentation for screen printed graphene ink. There is a possibility that the curve shows a similar trend, but the indentation and elastic behavior are not the same.

3.2.1 Characterization: Width and Pattern

Figure 15 demonstrates the graph of hardness values of the samples for 1 mm of width against five different points. Based on observation of the graph, a solid line that represents a straight line shows the highest average values except at points 1 and 5. Besides that, zigzag shows that the lowest average values of hardness between 0.06 HV to 0.50 HV (refer to Table 3). For sinusoidal and square, both line graphs show some similar trend except for point 1 and point 5. For Figure 16, it illustrates the graph line for 2 mm samples for hardness values against the point taken. This graph shows similar results as 1 mm samples as straight-line illustrates the highest average values of hardness while vice versa with a zigzag. Similar to 1 mm results, sinusoidal and square patterns maintain a moderate average value between the straight-line and zigzag. The highest value of hardness is at point 3 of sinusoidal which is 3.37 HV while the lowest value at point 3 of the square, which is 1.06 HV. On top of that, Figure 17 shows the graph pattern for 3 mm samples. Based on table 3, 3 mm samples show that the highest average values as compared to 1 mm and 2 mm samples. For 3 mm samples, they show some differences regarding the value as the highest average values of hardness are sinusoidal and follows by a straight line. Inversely, zigzag maintains as the lowest average values of hardness while the graph trend shows some fluctuating pattern. Overall, straight-line has the average hardness values, which vice versa with a zigzag. Other than that, 1 mm samples show the lowest average values from 0.10 HV to 0.80 HV. This is due to the straight-line is a simpler design as compared to the zigzag pattern.

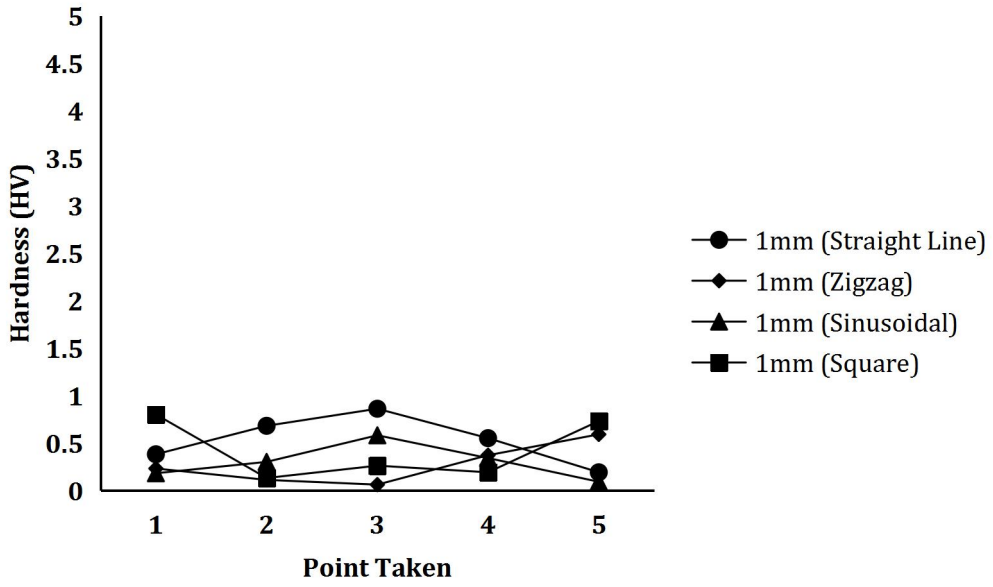

Figure 15. Sheet resistance against point taken (width: 1 mm).

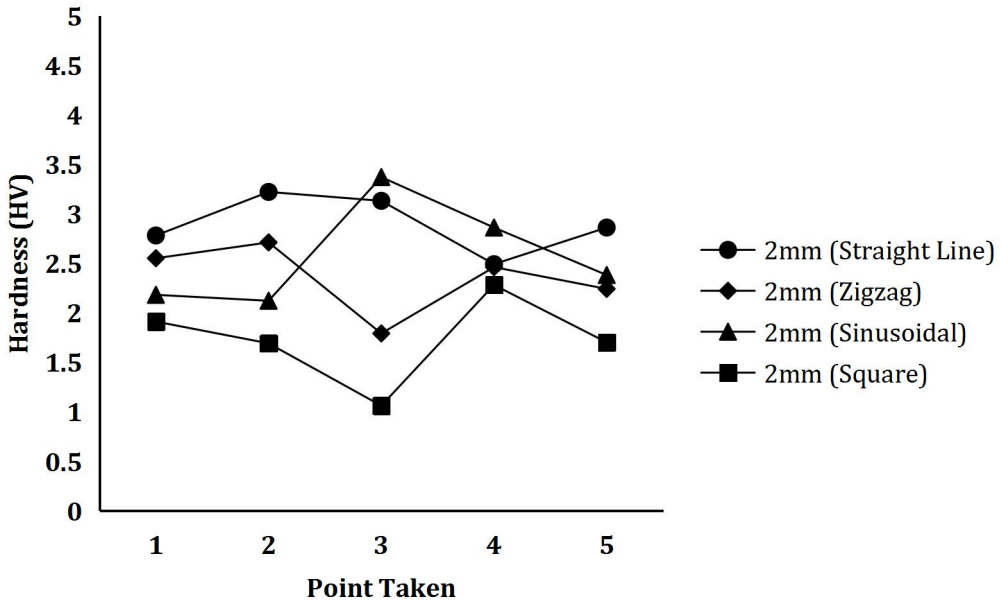

Figure 16. Sheet resistance against point taken (width: 2mm).

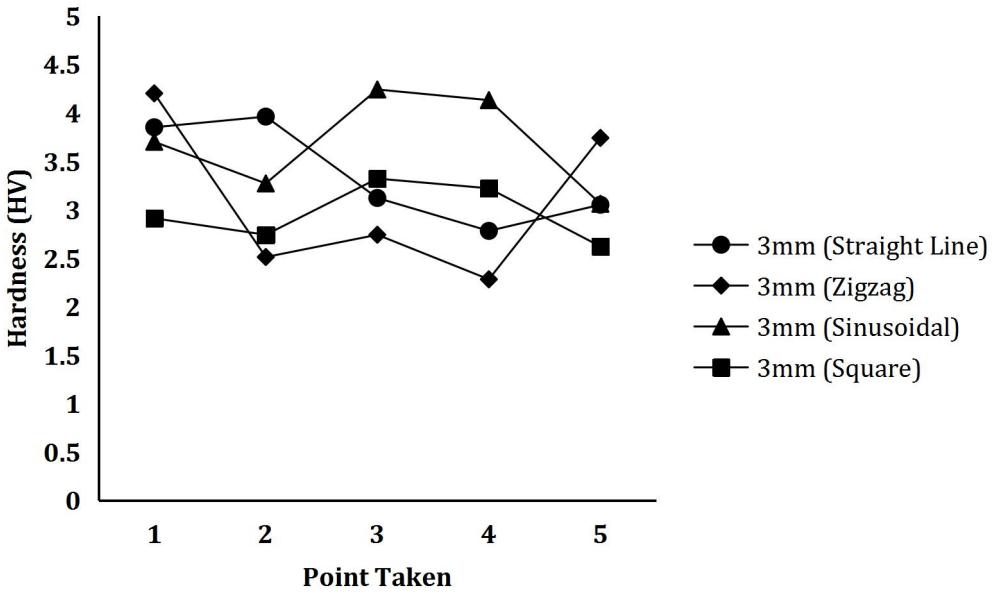

Figure 17. Sheet resistance against point taken (width: 3mm).

4. CONCLUSION

In conclusion, the present work had successfully fabricated graphene incorporated with epoxy resin and hardener, which acted as a composite for conductive ink. In order to produce the ink, the material preparation, printing process, and curing process were done. The results from the present work of testing had achieved all the objectives as described. Electrical properties show that the straight-line has the best properties in allowing the current to efficiently flow in contrast with a zigzag pattern. It also shows that the mechanical properties of the straight-line pattern and 3 mm of width is the best in enduring the force as compared to other patterns. Besides that, this study also concludes that 3 mm of width sample is the most suitable width for conductive ink as it shows better properties as compared to 2 mm and 1 mm. Further research needs to be carried out to prove that graphene is the best conductive material as the conductive ink filler, and to produce a low-cost conductive ink with the best properties of conductive materials.

ACKNOWLEDGEMENTS

Special thanks to the Advanced Manufacturing Centre (AMC) and Fakulti Kejuruteraan Mekanikal (FKM), Universiti Teknikal Malaysia Melaka (UTeM) for providing the laboratory facilities.

REFERENCES

[1] Magdassi, S., & Kamyshny, A. (Eds.). Nanomaterials for 2D and 3D Printing. *John Wiley & Sons*, (2017).

[2] Shrivas, K., Ghosale, A., Bajpai, P. K., Kant, T., Dewangan, K., & Shankar, R. Advances of flexible electronics and electrochemical sensors using conducting nanomaterials: A review. *Microchemical Journal*, (2020) 104944.

[3] Bacalzo Jr, N. P., Go, L. P., Querebillo, C. J., Hildebrandt, P., Limpoco, F. T., & Enriquez, E. P. Controlled microwave-hydrolyzed starch as a stabilizer for green formulation of

aqueous gold nanoparticle ink for flexible printed electronics. *ACS Applied Nano Materials*, **1**(3), (2018) pp.1247-1256.

[4] Xu, W., & Wang, T. Synergetic effect of blended alkylamines for copper complex ink to form conductive copper films. *Langmuir*, **33**(1), (2017) pp.82-90.

[5] Babaahmadi, V., Montazer, M., & Gao, W. Low temperature welding of graphene on PET with silver nanoparticles producing higher durable electro-conductive fabric. *Carbon*, **118**, (2017) pp.443-451.

[6] Xue, L., Wang, W., Guo, Y., Liu, G., & Wan, P. Flexible polyaniline/carbon nanotube nanocomposite film-based electronic gas sensors. *Sensors and Actuators B: Chemical*, **244**, (2017) pp.47-53.

[7] Nickels, L. Improving composites with 'wonder material'. *Reinforced Plastics*, **60**(4), (2016) pp.224-227.

[8] Bonaccorso, F., Sun, Z., Hasan, T. A., & Ferrari, A. C. Graphene photonics and optoelectronics. *Nature photonics*, **4**(9), (2010) pp.611.

[9] Liu, Z., Parvez, K., Li, R., Dong, R., Feng, X., & Müllen, K. Transparent conductive electrodes from graphene/PEDOT: PSS hybrid inks for ultrathin organic photodetectors. *Advanced Materials*, **27**(4), (2015) pp.669-675.

[10] Zhu, Z., & Chen, J. Advanced carbon-supported organic electrode materials for lithium (sodium)-ion batteries. *Journal of the Electrochemical Society*, **162**(14), (2015) A2393.

[11] Deb, J., Seriani, N., & Sarkar, U. Ultrahigh carrier mobility of penta-graphene: A first-principle study. *Physica E: Low-dimensional Systems and Nanostructures*, **127**, (2021) 114507.

[12] Secor, E. B., Prabhumirashi, P. L., Puntambekar, K., Geier, M. L., & Hersam, M. C. Inkjet printing of high conductivity, flexible graphene patterns. *The journal of physical chemistry letters*, **4**(8), (2013) pp.1347-1351.

[13] Tran, T. S., Dutta, N. K., & Choudhury, N. R. Graphene inks for printed flexible electronics: Graphene dispersions, ink formulations, printing techniques and applications. *Advances in colloid and interface science*, **261**, (2018) pp.41-61.

[14] Saidina, D. S. *Fabrication and Characterization of graphene-based ink for flexible electronic* (Doctoral dissertation, Université de Lorraine; Universiti Sains Malaysia (Malaisie)).

[15] Brennan, B., Spencer, S. J., Belsey, N. A., Faris, T., Cronin, H., Silva, S. R. P., ... & Pollard, A. J. Structural, chemical and electrical characterisation of conductive graphene-polymer composite films. *Applied Surface Science*, **403**, (2017) pp.403-412.

[16] Saad, H., Salim, M. A., Masripan, N. A., Saad, A. M., & Dai, F. Nanoscale Graphene Nanoparticles Conductive Ink Mechanical Performance Based on Nanoindentation Analysis. *International Journal of Nanoelectronics & Materials*, **13**, (2020).

[17] Deng, Z. Y., Yang, J. F., Beppu, Y., Ando, M., & Ohji, T. Effect of agglomeration on mechanical properties of porous zirconia fabricated by partial sintering. *Journal of the American Ceramic Society*, **85**(8), (2020) pp.1961-1965.

[18] Maizura, M., Mohd Azli, S., Nor Azmmi, M., Adzni, M., Mohd Nizam, S., Ghazali, O., & Caridi, F. Nanoindentation of graphene reinforced epoxy resin as a conductive ink for microelectronic packaging application. *International Journal of Nanoelectronics & Materials*, **13**, (2020).

[19] Ismail, N., Salim, M. A., Naroh, A., Saad, A. M., Masripan, N. A., Donik, C., ... & Dai, F. The Behaviour of Graphene Nanoplatelates Thin Film for High Cyclic Fatigue. *International Journal of Nanoelectronics & Materials*, **13**, (2020).

[20] Salim, M. A., Dai, F., Saad, A. M., Masripan, N. A., Dmitriev, A. N., Naroh, A., ... & Akop, M. Z. Prediction Effects on Internal Resonance Wave of Metallic Conductive Ink in Rotational Motion Behaviour. *International Journal of Nanoelectronics and Materials*, **13**, (2020) pp.295-304.